New Phytologist

Research

How adaptable is the hydraulic system of European beech in the face of climate change-related precipitation reduction?

Bernhard Schuldt[1]*, Florian Knutzen[1]*, Sylvain Delzon[2], Steven Jansen[3], Hilmar Müller-Haubold[1], Régis Burlett[2], Yann Clough[4] and Christoph Leuschner[1]

[1]Plant Ecology, Albrecht von Haller Institute for Plant Sciences, University of Göttingen, Untere Karspüle 2, 37073 Göttingen, Germany; [2]UMR BIOGECO INRA-UB, University of Bordeaux, Avenue des Facultés, 33405 Talence, France; [3]Institute for Systematic Botany and Ecology, Ulm University, Albert-Einstein-Allee 11, 89081 Ulm, Germany; [4]Centre for Environmental and Climate Research, Faculty of Science, Lund University, Sölvegatan 37, 223 62 Lund, Sweden

Author for correspondence:
Bernhard Schuldt
Tel: +49 551 39 22205
Email: bernhard.schuldt@plant-ecology.de

Received: *10 August 2015*
Accepted: *6 November 2015*

New Phytologist (2016) **210:** 443–458
doi: 10.1111/nph.13798

Key words: drought stress, functional trait, hydraulic conductivity, leaf morphology, pit membrane, precipitation gradient, vulnerability to cavitation, wood anatomy.

Summary

- Climate warming will increase the drought exposure of many forests world-wide. It is not well understood how trees adapt their hydraulic architecture to a long-term decrease in water availability.
- We examined 23 traits characterizing the hydraulic architecture and growth rate of branches and the dependent foliage of mature European beech (*Fagus sylvatica*) trees along a precipitation gradient (855–594 mm yr^{-1}) on uniform soil. A main goal was to identify traits that are associated with xylem efficiency, safety and growth.
- Our data demonstrate for the first time a linear increase in embolism resistance with climatic aridity (by 10%) across populations within a species. Simultaneously, vessel diameter declined by 7% and pit membrane thickness (T_m) increased by 15%. Although specific conductivity did not change, leaf-specific conductivity declined by 40% with decreasing precipitation. Of eight plant traits commonly associated with embolism resistance, only vessel density in combination with pathway redundancy and T_m were related.
- We did not confirm the widely assumed trade-off between xylem safety and efficiency but obtained evidence in support of a positive relationship between hydraulic efficiency and growth. We conclude that the branch hydraulic system of beech has a distinct adaptive potential to respond to a precipitation reduction as a result of the environmental control of embolism resistance.

Introduction

Most climate change scenarios for Central Europe predict a rise in mean annual temperature by 2.5–3.5°C for the end of the 21st Century (Rowell & Jones, 2006; Jacob *et al.*, 2008), an increasing frequency and raised intensity of summer heat waves (Schär *et al.*, 2004; Fischer & Schär, 2008) and a regional decrease in summer precipitation by up to 25% (Meinke *et al.*, 2010). These changes will probably affect forest productivity, which in many regions of Central Europe largely depends on water availability (Bréda *et al.*, 2006; Weber *et al.*, 2013). In regions with a rising frequency and severity of summer drought, the dependence of tree growth and vitality on water supply is therefore likely to increase in the future. Such a trend can also increase tree mortality through hydraulic failure (Anderegg *et al.*, 2015; McDowell & Allen, 2015), and it may eventually change tree species composition in natural forests as a result of differential species responses (Rigling *et al.*, 2013). A better understanding of drought effects on the vitality and productivity of important tree species is urgently needed.

The natural forest vegetation of Central Europe is dominated by a single species, European beech (*Fagus sylvatica*; Ellenberg & Leuschner, 2010), which would naturally cover almost 66% of the area of Germany (Bohn *et al.*, 2003). Although this species preferentially grows on well-drained, moist soils in oceanic to suboceanic climates, it occurs under widely different precipitation regimes (Ellenberg & Leuschner, 2010). Such a wide spectrum of hydrological site conditions can be colonized by a species if it maintains a high degree of genetic variability at the metapopulation level by producing genotypes with adaptation to moist or relatively dry habitats, or if a high phenotypic plasticity does exist which allows the individual to acclimatize to a broad range of hydrological conditions (Kremer *et al.*, 2014). However, it remains a matter of debate to what extent beech is threatened by increasing drought in the future, especially at its distributional margins (Jump *et al.*, 2006; Herbette *et al.*, 2010). In fact, the genotypic variation of drought tolerance and the drought acclimation potential are not sufficiently known for mature beech trees (Bolte *et al.*, 2007; Gessler *et al.*, 2007; Leuschner, 2009).

*These authors contributed equally to this work.

In beech, several traits have been identified that indicate a considerable sensitivity to drought, including a marked precipitation sensitivity of radial growth (Weber *et al.*, 2013; Zimmermann *et al.*, 2015). Common-garden experiments with seedlings from several European beech provenances, however, demonstrate a pronounced adaptability of the hydraulic system. While wood anatomical traits seem partly to be under genetic control (Eilmann *et al.*, 2014), embolism resistance is uncoupled from genetic differentiation and appears to be mainly under environmental control building on phenotypic plasticity (Wortemann *et al.*, 2011; Aranda *et al.*, 2015). However, the degree of phenotypic variability in hydraulic traits has never been quantified in European beech and corresponding information is needed in particular for adult trees across gradients of water availability.

To date, only a few studies have investigated the synchronous variation of xylem anatomy, hydraulic properties and leaf traits within a single tree species across environmental gradients (Anderegg & Meinzer, 2015). Consequently, less is known about intraspecific variation in hydraulic traits than interspecific variation, despite the importance of the former for predicting tree responses to climate change (Anderegg, 2015). This is somewhat surprising given the long-standing understanding that wood anatomical diversity is induced by environmental factors and influenced by the capacity to withstand drought (Vesque, 1876; Carlquist, 1966). Several studies on intraspecific variation in hydraulic properties have demonstrated a strong precipitation effect on conduit traits (Chenlemuge *et al.*, 2015; Schreiber *et al.*, 2015) as a consequence of either genetic variability or phenotypic plasticity. Consequently, a central role in hydraulic efficiency and safety is played by average vessel size and vessel size distribution (Tyree *et al.*, 1994). Furthermore, wood anatomical and derived hydraulic properties are directly related to growth (Hajek *et al.*, 2014; Hoeber *et al.*, 2014; Kotowska *et al.*, 2015), demonstrating the close relationship between plant hydraulic conductance and productivity (Tyree, 2003). However, it has repeatedly been demonstrated that decreasing precipitation causes narrower conduits and higher conduit densities, both across and within species (Carlquist, 1977; Lens *et al.*, 2004; Sterck *et al.*, 2008; Gleason *et al.*, 2012; Chenlemuge *et al.*, 2015). When comparing various species, this pattern generally leads to increased embolism resistance, while within-species comparisons have yielded mixed results (Martinez-Vilalta *et al.*, 2009; Herbette *et al.*, 2010; Wortemann *et al.*, 2011; Sterck *et al.*, 2012). It is generally accepted that air-seeding is the primary cause of cavitation and thus embolism formation, subsequently rupturing the water column and causing water transport failure (Tyree & Zimmermann, 2002). The consequences are stomatal closure and reduced carbon assimilation. In the past, several traits have been related to embolism resistance with mixed results, among them wood density (Hacke *et al.*, 2001; Jacobsen *et al.*, 2007; Martinez-Vilalta *et al.*, 2009; Gleason *et al.*, 2016), vessel size (Carlquist, 1977; Tyree *et al.*, 1994; Maherali *et al.*, 2006; Hajek *et al.*, 2014), vessel density (Lens *et al.*, 2011; Ogasa *et al.*, 2013), hydraulic conductivity (Maherali *et al.*, 2006; Markesteijn *et al.*, 2011; Gleason *et al.*, 2016), vessel grouping (Loepfe *et al.*, 2007; Lens *et al.*, 2011; Carlquist, 2012), pit structure (Wheeler *et al.*, 2005; Jansen *et al.*, 2009a; Plavcová *et al.*, 2013; Bouche *et al.*, 2014), sapwood-to-leaf area ratio (Willson *et al.*, 2008; Sterck *et al.*, 2012; Schreiber *et al.*, 2015) and specific leaf area (Maherali *et al.*, 2006; Fan *et al.*, 2011; Markesteijn *et al.*, 2011); a number of these traits are at least partly interrelated.

Precipitation gradients represent a valuable tool for investigating the short-term acclimation (plasticity) of mature trees to a decrease in rainfall when the edaphic conditions and stand structure are sufficiently uniform across the stands. Here, we investigate acclimation in the branch hydraulic system of mature beech trees in five stands on uniform sandy soil across a 130-km-long gradient of *c.* 260 mm yr^{-1} difference in mean annual precipitation. The low end of the gradient was close to the known drought limit of beech. We combined anatomical and hydraulic measurements in sun-canopy branches with the examination of foliar properties addressing 20 parameters in total and related these traits to three common measures of embolism resistance.

The main goal of this study in mature European beech trees was to identify morphological and physiological traits that are associated with xylem efficiency, safety and growth in trees of comparable age and size growing along a precipitation gradient on uniform soil. The main hypotheses tested were that (i) vessel diameter and hydraulic efficiency decrease with a lasting reduction in precipitation while (ii) embolism resistance increases, and that (iii) branch growth rate trades off with both hydraulic efficiency and safety.

Materials and Methods

Study sites and microclimatic conditions

The study was carried out in five mature beech (*Fagus sylvatica* L.) stands of similar age and structure along a precipitation gradient in the Pleistocene lowlands of north-western Germany in 2011. The precipitation gradient covers a 130-km-long northwest–southeast transect from the east of the state of Lower Saxony to the western part of Saxony-Anhalt and includes a climatic gradient from a suboceanic to a subcontinental climate with a continuous long-term (1981–2010) mean annual precipitation (MAP) decrease from 855 to 594 mm yr^{-1}, a decrease in mean annual early summer growing season (April-June)precipitation (MSP) from 188 to 147 mm yr^{-1} and a mean annual temperature (MAT) increase from 8.5 to 9.1°C (Table 1). Climatic data were obtained from a 1 × 1 km^2 grid data set (Deutscher Wetterdienst, Offenbach, Germany). We additionally calculated a simplified forest aridity index (FAI) according to Führer *et al.* (2011) as $FAI = 100 \times T_{Jul–Aug}/(P_{May–Jul} + P_{Jul–Aug})$, where T is the temperature and P the precipitation of the associated interval. As the atmospheric evaporative demand in the growing season is highest in midsummer (July and August), the July precipitation was weighted by a factor of two in the denominator. This index has been developed for the comparison of different beech stands in southeast Europe; FAI values in the distribution range of beech are generally < 4.75 (Führer *et al.*, 2011).

All five sites were situated on highly acidic and nutrient-poor sandy soils developed in fluvioglacial sands or moraine deposits

Table 1 Stand characteristics of the five investigated beech (*Fagus sylvatica*) forests along a precipitation gradient in northwest Germany

Site	Code	Symbol	MAP	MSP	MAT	FAI	DBH	*H*	n_{tree}	n_{sample}
Calvörde	Ca	●	593.91	146.75	9.3 ± 1.9	6.19	37.42 ± 2.47	25.82 ± 0.18	5	13–17
Klötze	Kl	●	654.76	157.30	9.1 ± 1.9	5.60	42.36 ± 3.65	29.71 ± 0.29	5	14–16
Göhrde	Go	●	707.11	164.57	9.0 ± 1.8	5.15	40.13 ± 2.00	24.20 ± 1.14	5	16–19
Unterlüß	Un	●	816.06	175.96	8.7 ± 1.8	4.86	40.83 ± 3.07	22.27 ± 1.10	5	16–18
Sellhorn	Se	●	855.37	188.14	8.7 ± 1.8	4.53	39.79 ± 2.43	28.93 ± 1.04	5	14–17

Given are the site codes and symbol colours, mean annual precipitation (MAP; mm yr^{-1}) and mean early summer growing season (April–June) precipitation (MSP; mm) for the period 1981–2010, mean annual temperature (MAT; °C), the forest aridity index (FAI), the average diameter at breast height (DBH; cm), tree height (*H*; m) and the numbers of tree individuals measured (n_{tree}) and samples per site (including pseudoreplicates; n_{sample}). Values are mean ± SE. The sample numbers for wood density and transmission electron microscopy measurements are not given here; see the corresponding Materials and Methods section.

of the penultimate Ice Age (Saalian) covered by periglacial drift sand. Mean (± SE) tree age was 104.6 ± 6.7 yr. For detailed information on stand structure and climatic parameters at the five study sites, see Müller-Haubold *et al.* (2013) and Hertel *et al.* (2013). Some structural data on the individual beech trees investigated are given in Table 1.

Tree selection and plant material

Five mature beech trees of similar size and canopy position within a particular stand were selected at the five sites and branch and twig samples collected from the uppermost sun-exposed crown with tree-climbing equipment in August 2011. Per tree, five twigs of *c.* 50 cm length were air-cut and immediately transferred to polyethylene tubes filled with water containing a sodium-silver-chloride complex (16 μg l^{-1} silver (Ag) and 8 mg l^{-1} NaCl; Micropur katadyn, Wallisellen, Switzerland) to prevent microbial growth and stored at 4°C. Across the gradient, all branches were more or less of comparable size and age, although a certain variation in sapwood area at a given branch age was unavoidable (Supporting Information Fig. S1). Additionally, all leaves distal to the sampled twig segments were harvested. For wood density determination, three large branch wood samples were collected from the uppermost canopy of a tree. A list of all traits measured, the corresponding acronyms and units is given in Table 2.

Wood density

Wood density (WD; g cm^{-3}) was determined for three branch wood samples per tree (mean diameter ± SE: 3.09 ± 0.07 cm; mean length ± SE: 15.15 ± 0.43 cm), yielding 64 samples in total. Fresh volume was gravimetrically measured at a precision of 10 mg after removing pith and bark by water displacement according to Archimedes' principle and branch samples subsequently oven-dried at 105°C for 72 h.

Hydraulic conductivity and vulnerability curves

Hydraulic properties were measured for three to five samples per tree, yielding 78 samples in total. Branch segments were shortened to *c.* 28 cm length (mean basipetal diameter ± SE: 8.04 ± 0.11 mm), lateral branches were cut off, scars were sealed with quick-drying superglue (Loctite 431; Henkel, Düsseldorf, Germany) and the segments were connected to the Xyl'em apparatus (Bronkhorst, Montigny les Cormeilles, France). Segments were flushed three times for 10 min at a pressure of 120 kPa with filtered (0.2 μm) and degased demineralized water (10 mM KCl and 1 mM $CaCl_2$) and maximum hydraulic conductivity (K_h; kg m MPa^{-1} s^{-1}) was recorded along a 6-kPa pressure difference. The diameter of each segment was measured twice at the basipetal and distal ends, and at four positions along the segment. In order to calculate specific conductivity (K_S; kg m^{-1} MPa^{-1} s^{-1}) normalized by sapwood area, a regression analysis between total cross-sectional area (A_{cross}; mm^2) and corresponding xylem cross-sectional area (A_{xylem}; mm^2) was carried out assuming that all rings were still functional. From each segment, high-quality top-view images from the planed thick and thin ends were analysed for A_{cross} and A_{xylem} with the software ImageJ (v.1.44p; http://rsb.info.nih.gov/ij). The following regression coefficients were used to calculate sapwood area without pith and bark for a given segment diameter: $A_{xylem} = -3.715 + 0.770\ A_{cross}$ ($P < 0.001$; $r^2 = 0.98$; $n = 238$). According to linear regression analyses, K_h divided by the maximal basipetal sapwood area revealed the strongest relationships (Table S1). This pattern was documented in Hajek *et al.* (2014) and Hoeber *et al.* (2014). Leaf-specific conductivity (K_L; kg m^{-1} MPa^{-1} s^{-1}) was calculated by dividing K_h by the total supported leaf area distal to the branch segment (A_{leaf}; cm^2).

Subsequently, branch segments were inserted into a honeycomb custom-made rotor (Delzon *et al.*, 2010) of the Cavitron (Cochard *et al.*, 2005) attached to a commercially available centrifuge (Sorvall RC-5C; Thermo Fisher Scientific, Waltham, MA, USA). Conductivity measurements started at 1.0 MPa and were repeated stepwise at intervals of 0.2–0.3 MPa until the percent loss of conductivity (PLC) reached at least 90%. Vulnerability curves were generated by plotting PLC against xylem pressure (Fig. 1), and the pressure causing 50% loss of conductivity (P_{50}) was calculated according to a sigmoidal function (Pammenter & Vander Willigen, 1998) as $PLC = 100/(1 + \exp(s/25 \times (P_i - P_{50})))$, where *s* (% MPa^{-1}) is the negative slope of the curve at the inflexion point and P_i the xylem pressure. The xylem pressures causing 12% (P_{12}; air entry point) and 88% (P_{88}) loss of conductivity were also

Table 2 List of variables included in the study, with definitions and units

Abbreviation	Units	Definition
Environmental conditions		
MAP	mm yr^{-1}	Long-term mean annual precipitation
MSP	mm yr^{-1}	Long-term mean annual early summer growing season precipitation
MAT	°C	Long-term mean annual temperature
FAI		Forest aridity index
Structural parameters		
H	m	Tree height
DBH	cm	Diameter at breast height
BA	yr	Branch age
Hydraulic traits		
K_S	kg m^{-1} MPa^{-1} s^{-1}	Specific conductivity
K_P	kg m^{-1} MPa^{-1} s^{-1}	Potential conductivity
K_L	10^{-4} kg m^{-1} MPa^{-1} s^{-1}	Leaf-specific conductivity
P_{12}	MPa	Xylem pressure at 12% loss of hydraulic conductance
P_{50}	MPa	Xylem pressure at 50% loss of hydraulic conductance
P_{88}	MPa	Xylem pressure at 88% loss of hydraulic conductance
Wood properties		
WD	g cm^{-3}	Branch wood density
D	µm	Vessel diameter
D_h	µm	Hydraulically weighted vessel diameter
VD	n mm^{-2}	Vessel density
VI	mm m^{-2}	Carlquist's vulnerability index
V_G		Vessel grouping index
V_S		Solitary vessel index
T_m	nm	Intervessel pit membrane thickness
T_w	µm	Intervessel wall thickness
A_{xylem}	mm^2	Branch sapwood area
A_{xylem} : A_{leaf}	10^{-4} m^2 m^{-2}	Sapwood to leaf area ratio (Huber value)
A_{lumen} : A_{xylem}	%	Relative vessel lumen area (lumen to sapwood area ratio)
G_{dw}	mg m^{-1} yr^{-1}	Branch growth rate
Foliar traits		
LS	cm^2	Mean leaf size
SLA	cm^2 g^{-1}	Specific leaf area
$\delta^{13}C$	‰	Carbon isotope signature

calculated following Domec & Gartner (2001) as $P_{12} = 2/(s/25) + P_{50}$ and $P_{88} = -2/(s/25) + P_{50}$.

Wood anatomy, potential conductivity and branch growth rate

Branch segments from the basipetal end were used for wood anatomical investigation, yielding 77 samples in total. Transverse sections cut with a sliding microtome (G.S.L.1; Schenkung Dapples, Zurich, Switzerland) were digitalized at ×100 magnification using a stereomicroscope equipped with a digital camera (SteREOV20; Carl Zeiss MicroImaging GmbH, Göttingen, Germany). Image processing was performed with the software Adobe Photoshop CS6 (v.13.0.1; Adobe Systems Inc., San Jose, CA, USA) and ImageJ using the particle analysis function to

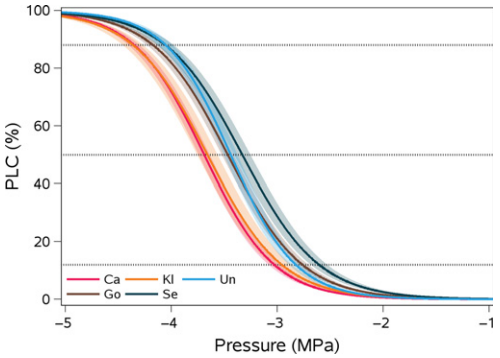

Fig. 1 Mean vulnerability curves for the five beech (*Fagus sylvatica*) forests differing in water availability showing xylem pressure in relationship to percentage loss of hydraulic conductance (PLC). The curves shown have been averaged for all samples per tree and subsequently across the five trees, 16 per site. For site abbreviations, see Table 1. The shaded band represents the SD. Different colours indicate differences in water availability.

estimate single and cumulative vessel lumen area (A_{lumen}; m^2), vessel density (VD; n mm^{-2}) and vessel diameter (D; µm) from major (a) and minor (b) vessel radii according to the equation given by Lewis & Boose (1995) as $D = ((32 \times (a \times b)^3)/(a^2 + b^2))^{1/4}$ and used to calculate the hydraulically weighted diameter (D_h; µm) according to Sperry *et al.* (1994) as $D_h = \Sigma D^5/\Sigma D^4$. Relative vessel lumen area (A_{lumen} : A_{xylem}; %) was calculated by dividing cumulative vessel lumen area (A_{lumen}; m^2) by the corresponding sapwood area (A_{xylem}; m^2). Carlquist's vulnerability index (VI) (Carlquist, 1977), which is commonly used to indicate a species' adaptation to xeric or mesic conditions (De Micco *et al.*, 2008), was calculated as $VI = (D/1000)/(VD/1000\,000)$. The vessel grouping index (V_G) was estimated by dividing the total number of vessels by the number of grouped vessels, and the solitary vessel index (V_S) by dividing the number of solitary vessels by the total number of vessels; for these calculations, a subsample of 216.4 ± 5.6 vessels (mean ± SE) were measured per branch sample, with both solitary vessels and grouped vessels considered as a vessel group (Scholz *et al.*, 2013). For all calculations (except for V_G and V_S), the complete cross-section was analysed, yielding 3537–30 989 measured vessels per branch sample. For V_G and V_S, pie slices from the cross-section were used, yielding 110–379 measured vessels per sample. Potential conductivity (K_P; kg m^{-1} MPa^{-1} s^{-1}) was calculated according to the Hagen–Poiseuille equation as $K_P = (((\pi \times \Sigma D^4)/128\,\eta) \times \rho)/A_{xylem}$, where η is the viscosity ($1.002\ 10^{-9}$ MPa s) and ρ the density of water (998.2 kg m^{-3}), both at 20°C, and A_{xylem} (m^2) is the analysed sapwood area. Additionally, the relative abundance of vessels in five vessels size classes was calculated by dividing the number of vessels in a class by the total vessel number.

We further calculated branch growth rate (G_{dw}; mg m^{-1} yr^{-1}) according to Sterck *et al.* (2012) as $G_{dw} = BAI \times WD \times 10^{-6}$, where BAI is the average annual basal area increment (m^2 yr^{-1}) and WD the corresponding wood density (kg m^{-3}). BAI was calculated by analysing the area of each growth ring separately, yielding 451 analysed growth rings in total.

Transmission electron microscopy

A subsample of three to four branch segments from each of three trees per site was used for transmission electron microscopy (TEM) observations of intervessel pit membrane thickness (T_m; nm) and intervessel wall thickness (T_w; nm), yielding 18 samples in total. Samples were stored in 70% ethanol, and were from the same branches that were used to construct vulnerability curves and for wood anatomical measurements. Samples were prefixed in a standard solution (2.5% glutaraldehyde, 0.1 mol phosphate and 1% saccharose, pH 7.3) and prepared according to a standard TEM protocol (Jansen *et al.*, 2009b). Ultrathin, transverse sections were observed with a JEOL 1400 transmission electron microscope (JEOL Ltd, Tokyo, Japan). The conduit size and general morphology of bordered pits were used to distinguish intervessel pit membranes from vessel–tracheid or tracheid–tracheid pit membranes. Given the morphological continuum between vessel elements and tracheids, the exact nature of conduits could not always be distinguished. Therefore, TEM measurements were only included in our analyses when the vessel identity was clear.

Leaf morphology

All leaves distal to the twig segments used for hydraulic conductivity measurements were stripped off and scanned for determination of single and cumulative leaf areas (WinFolia 2005; Régent Instruments, Quebec City, QC, Canada). Per branch segment, eight to 132 leaves were scanned, yielding 5464 leaves in total. The average leaf size (LS; cm^2) was determined by dividing the total leaf area by the number of leaves per branch, and the Huber value, that is, the sapwood-to-leaf-area ratio ($A_{xylem}:A_{leaf}$; $10^{-4}\ m^2\ m^{-2}$), was calculated by dividing the sapwood area determined according to the linear regression analysis mentioned under hydraulic conductivity and vulnerability curves by the corresponding total leaf area (A_{leaf}; cm^2). Subsequently, leaves were oven-dried at 70°C for 48 h in order to determine the specific leaf area (SLA; $cm^2\ g^{-1}$). The carbon isotope signature ($\delta^{13}C$) of the leaf dry mass was analysed by mass ratio spectroscopy (Deltaplus; ThermoFinnigan, Bremen, Germany) at the Centre for Stable Isotope Research and Analysis (KOSI), University of Göttingen.

Statistical analyses

The trait variables investigated are summarized in Table 2. Our approach and the labour-intensive process of gaining access to the uppermost canopy using tree-climbing equipment forced us to apply a nested design, that is, three to five samples were taken per tree, but only five trees were analysed per site.

All statistical analyses were performed with the software package R (R Development Core Team 2013, version 3.0.0) except for linear regression analyses which were executed with the software XACT 8.03 (SciLab, Hamburg, Germany). All variables were tested for normality with a Shapiro–Wilk normality test and log-transformed if required. Linear mixed effect (LME) models with FAI, MAP or MSP as a fixed variable were used to test for significant differences in all trait variables along the rainfall gradient. We assumed nonindependence of different samples within a tree and of different trees within a plot in the models by adding plot and tree nested in plot as random effects. For investigating relationships between trait variables, Pearson correlation analyses were carried out on the tree level.

To search for patterns of interrelationships among the examined 23 traits, a principal components analysis (PCA) was conducted with plot-level means using the software package CANOCO (v.5.02; Biometris, Wageningen, the Netherlands) with all functional traits centred and standardized before analysis. Although our number of variables exceeded the number of plots by far, the first few eigenvectors are little affected when the matrix is not of full rank and do not lead to incorrect interpretations of ordinations in reduced space (Legendre & Legendre, 1998).

Results

Variation in functional traits along the precipitation gradient

Across our gradient, MAP declined by 261 mm yr^{-1} while MSP (from April to June) declined by 41 mm. Changes in precipitation and the increase in MAT by 0.4°C from the wet to the dry end were additionally mirrored in the FAI, which increased by 1.66 (Table 1).

According to the LME models, only five of the 23 structural, hydraulic, wood anatomical and foliar traits were significantly related to the three measures of water availability, MAP, MSP and FAI (Table 3). A key result is that xylem safety increased linearly with an increase in climatic aridity (Fig. 2a). The three measures of embolism resistance (P_{12}, P_{50} and P_{88}) differed in their responses, with P_{12} showing the strongest decrease with a reduction in MAP (by 15% or 0.44 MPa), followed by P_{50} (by 10% or 0.33 MPa), while P_{88} was the least modified trait (by 5% or 0.23 MPa; Fig. 1; Table S2). The increase in hydraulic safety towards the drier sites was not associated with a decline in xylem efficiency measured as specific (K_S; Fig. 2b) or potential conductivity (K_P; Table 3), even though the highest conductivities were observed at the wettest site, Sellhorn (Se; Table S2). In contrast to K_S, K_L was strongly influenced by changes in MAP and declined by 40% towards the dry end of the gradient (Fig. 2c).

WD did not vary significantly along the gradient (Fig. 2d), and of all wood properties examined only D was significantly related to both FAI and MSP (and at marginal significance to MAP; $P < 0.10$; Table 3). From the wet to the dry end of the gradient, average D declined by 7% (i.e. by 1.3 μm) (Figs 2e, 3a) as a result of changes in the abundance of vessels in the two size classes 10–20 μm ($D_{10–20\ \mu m}$; increase by 10%) and 20–30 μm ($D_{20–30\ \mu m}$; decline by 10%; Fig. 3b), while the abundance of vessels in the other three size classes was unaffected by the precipitation level (Table S3). As a consequence, D_h did not vary across the gradient (Tables 3, S2), which contrasts with the decrease in D.

None of the parameters related to vessel distribution, that is, VD (Fig. 2f), V_G (Fig. 2g), V_S and VI, was altered in response to the precipitation decrease (Table 3). By contrast, T_m increased by

Table 3 Results of linear mixed effect models examining the influence of forest aridity index (FAI), mean annual precipitation (MAP) and mean early growing season precipitation (MSP) as fixed variables on the 23 measured parameters in European beech (*Fagus sylvatica*)

	FAI			MAP			MSP		
Variable	Δ_i	LR	*P*	Δ_i	LR	*P*	Δ_i	LR	*P*
Structural parameters									
BA	1.95	0.05	0.81	1.75	0.25	0.62	1.65	0.35	0.55
Hydraulic traits									
K_S	1.41	0.59	0.44	1.04	0.96	0.33	0.72	1.28	0.26
K_P	1.35	0.65	0.42	1.64	0.36	0.55	1.28	0.72	0.39
K_L	2.99	4.99	**0.03**	2.91	4.91	**0.03**	1.83	3.83	**0.05**
P_{12}	5.02	7.02	**0.01**	4.10	6.10	**0.01**	4.97	6.97	**0.01**
P_{50}	4.72	6.72	**0.01**	4.60	6.60	**0.01**	4.57	6.57	**0.01**
P_{88}	2.19	4.19	**0.04**	2.65	4.65	**0.03**	2.03	4.03	**0.04**
Wood properties									
WD	1.87	0.13	0.72	1.69	0.31	0.58	1.58	0.42	0.51
D	1.84	3.84	**0.05**	1.55	3.55	***0.06***	2.48	4.48	**0.03**
D_h	1.73	0.27	0.60	1.87	0.13	0.72	1.63	0.37	0.55
VD	0.20	1.80	0.18	0.19	2.19	0.14	0.51	2.51	0.11
VI	0.56	2.56	0.11	0.98	2.98	***0.08***	1.46	3.46	***0.06***
V_G	1.24	0.76	0.38	1.55	0.45	0.50	1.15	0.85	0.36
V_S	1.24	0.76	0.38	1.59	0.41	0.52	1.21	0.79	0.37
T_m	0.27	1.73	0.19	0.20	1.63	0.20	0.30	1.70	0.19
T_w	1.97	0.03	0.87	0.20	0.04	0.84	1.95	0.05	0.82
A_{xylem}	1.84	0.16	0.69	1.96	0.04	0.83	1.98	0.02	0.90
$A_{xylem} : A_{leaf}$	0.36	1.64	0.20	0.09	2.09	0.15	0.74	1.26	0.26
$A_{lumen} : A_{xylem}$	1.77	0.23	0.63	1.94	0.06	0.80	1.87	0.13	0.72
G_{dw}	1.78	0.22	0.64	1.97	0.03	0.86	1.98	0.02	0.88
Foliar traits									
LS	1.50	3.50	***0.06***	1.24	3.24	***0.07***	0.42	2.42	0.12
SLA	0.92	1.08	0.30	0.74	1.26	0.26	0.83	1.17	0.28
$\delta^{13}C$	1.09	0.91	0.34	0.31	1.69	0.19	0.44	1.56	0.21

Given are the delta Akaike information criterion (Δ_i), the likelihood ratio (LR) and probability of error (*P*-value); for abbreviations, see Table 2. Significant correlations ($P < 0.05$) are shown in bold, and marginally significant correlations ($P < 0.10$) in italic bold.

15% with increasing climatic aridity (Fig. 2h), while T_w remained unchanged (Table 3). The strong negative relationship between MAP and T_m according to the linear regression analysis could, however, not be confirmed by the LME models (Table 3), presumably because of the low sample number and thus high variation within two of the five sites (Table S2). Neither branch growth rate (G_{dw}) nor the lumen to sapwood area ratio ($A_{lumen} : A_{xylem}$) or $A_{xylem} : A_{leaf}$ was significantly related to the precipitation decrease.

The precipitation gradient had a surprisingly small effect on the sun canopy leaves of the beech trees: neither SLA nor the foliar carbon isotope signature ($\delta^{13}C$) changed along the gradient, suggesting that higher climatic aridity did not lead to stomatal closure. However, we found a trend to larger leaf sizes at the drier sites, contrary to expectation ($P < 0.10$; Fig. 2i).

Determinants of hydraulic efficiency and branch growth

At the tree level, the variation in K_L was caused by alteration of the $A_{xylem} : A_{leaf}$ ratio ($P < 0.001$; $r = 0.60$) and, to a lesser extent, with modification of *D* ($P < 0.05$; $r = 0.41$), but K_L showed no relationship to VD, D_h or K_S (Table 4). Differences in K_S, by contrast, were mainly driven by changes in *D* (Fig. 4a) and not by VD (Fig. 4d). In contrast to K_S, wood density was unrelated to *D* (Fig. 4b) but closely associated with VD (Fig. 4e). We further could confirm the commonly assumed trade-off between hydraulic efficiency and growth; fast-growing branches possessed a more efficient hydraulic system composed of larger (Fig. 4c) but fewer vessels (Fig. 4f) as compared with slower growing branches, and a significant positive relationship existed between G_{dw} and both K_S and K_P ($P < 0.05$; $r = 0.44$), but there was also a significant negative relationship with WD ($P < 0.05$; $r = 0.40$; Table 4). Furthermore, G_{dw} was negatively related to branch age (BA; $P < 0.001$; $r = 0.64$) and LS ($P < 0.01$; $r = 0.48$), and positively to $\delta^{13}C$ ($P < 0.05$; $r = 0.35$), indicating that younger branches grew faster at the cost of more frequent stomatal closure. This finding is further supported by the negative relationship between BA and K_S ($P < 0.01$; $r = 0.52$), and the absence of any relationship between BA and WD (Table 4).

Determinants of embolism resistance

At the tree level, only two of eight examined traits commonly associated with embolism resistance (K_S or K_L, WD, *D*, VD, V_G, T_m, $A_{xylem} : A_{leaf}$ and SLA) were found to be related to embolism resistance in our study (Table 4). Contrary to expectation, neither hydraulic efficiency (K_S and K_L) nor *D* decreased with increasing embolism resistance, indicating that a clear trade-off between

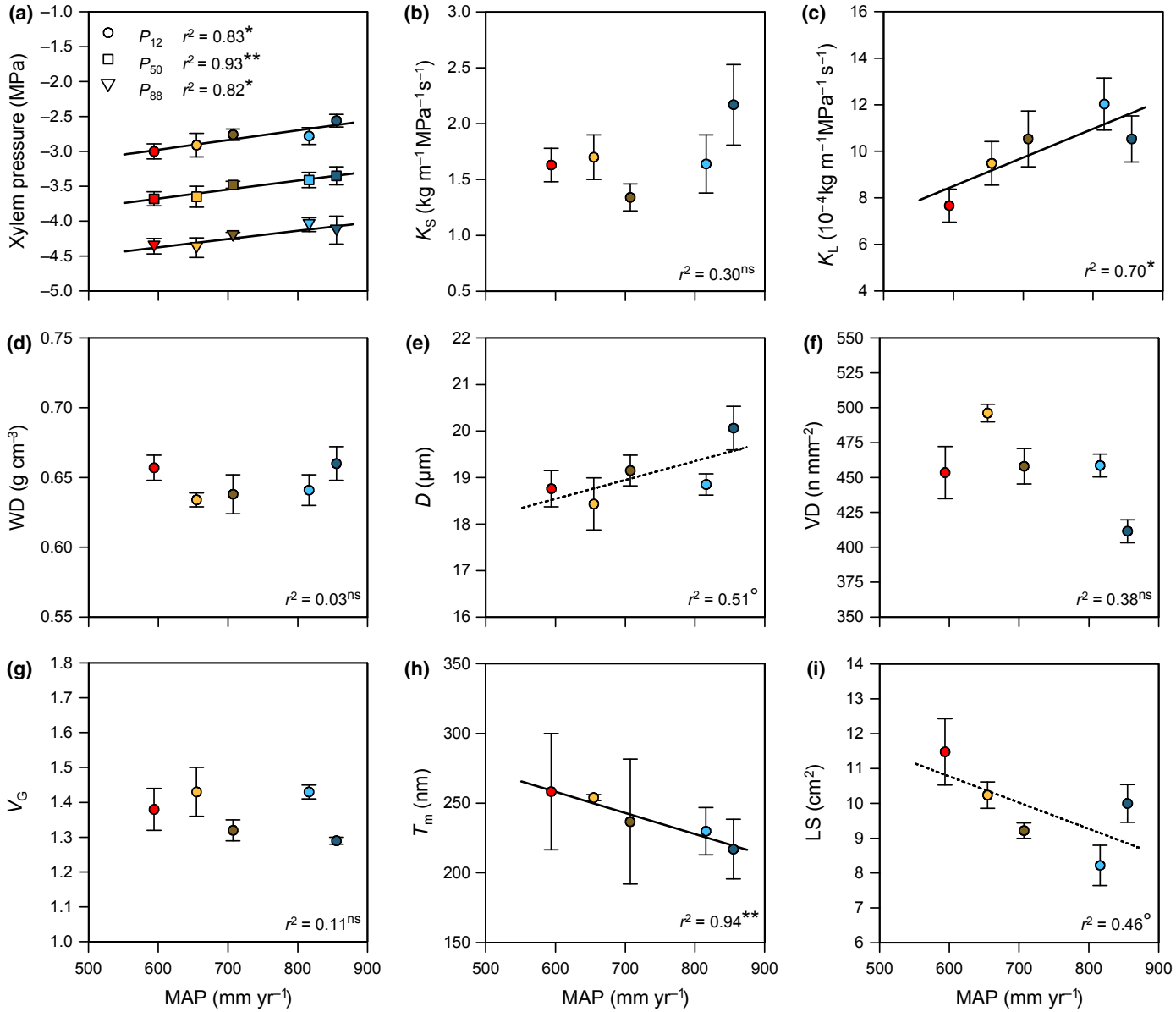

Fig. 2 Mean annual precipitation (MAP) in relation to (a) the xylem pressure causing 12, 50 or 88% loss of hydraulic conductance (P_{12}, P_{50} and P_{88}, respectively), (b) specific conductivity (K_S), (c) leaf-specific conductivity (K_L), (d) wood density (WD), (e) vessel diameter (D), (f) vessel density (VD), (g) vessel grouping index (V_G), (h) intervessel pit membrane thickness (T_m) and (i) mean leaf size (LS) in European beech (*Fagus sylvatica*). Values are mean ± SE per site; asterisks indicate the level of significance (°, $P < 0.10$; *, $P < 0.05$; **, $P < 0.01$; ns, nonsignificant relationships). For explanations of symbol colours, see Table 1.

hydraulic efficiency and safety does not exist in European beech. However, both VD and T_m were negatively related to embolism resistance, with VD showing a closer relationship to the air-entry point at high pressure (P_{12}; $P < 0.01$; $r = 0.46$) than to the P_{50} value ($P < 0.05$; $r = 0.34$), while T_m was most strongly associated with P_{88} ($P < 0.05$; $r = 0.56$), that is, the full embolism point at low pressure, and less strongly to P_{50} ($P < 0.10$; $r = 0.40$). Increased embolism resistance is achieved by the beech trees along the gradient by producing more vessels arranged in distinct groups but not necessarily by reducing vessel diameter (Fig. 5a); this is indicated by the positive relationship between VD and V_G (Fig. 5b). This finding is supported by a negative relationship between V_G and P_{12} at marginal significance ($P < 0.10$; $r = 0.28$). These adjustments in the vascular system apparently allowed trees to maintain a favourable leaf water status at the drier sites, as indicated by the negative relationship between VD and $\delta^{13}C$ (Fig. 5c), that is, a higher vessel density decreased the need to reduce leaf conductance.

The Pearson correlation analysis revealed several relationships between embolism resistance and morphological and growth-related parameters that were to some extent unexpected: BA was positively related to P_{50} ($P < 0.05$; $r = 0.34$; Table 4, Fig. S2b) and P_{88} ($P < 0.01$; $r = 0.49$), and branch size (A_{xylem}) was positively associated with P_{12} ($P < 0.05$; $r = 0.37$), P_{50} ($P < 0.01$;

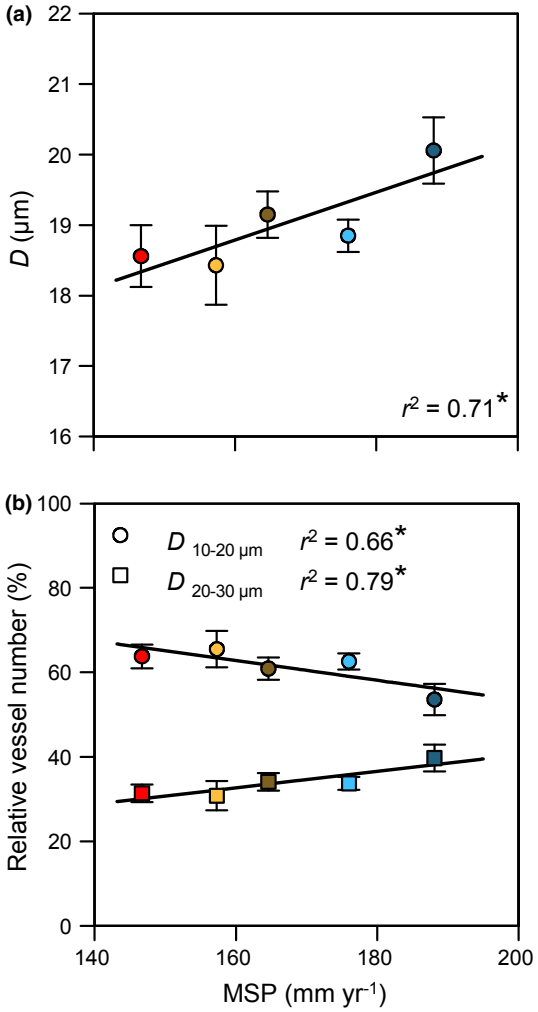

Fig. 3 (a) Vessel diameter (D) and (b) percentage of vessels relative to the total number of vessels diameter, classes 10–20 µm and 20–30 µm, in dependence on mean early summer growing season precipitation (MSP) in European beech (*Fagus sylvatica*). Values are mean ± SE per site. Asterisks indicate the level of significance (*, $P < 0.05$). For explanations of symbol colours, see Table 1.

$r = 0.47$) and P_{88} ($P < 0.01$; $r = 0.49$; Table 4). G_{dw} as a measure of productivity was negatively related to P_{88} ($P < 0.05$; $r = 0.34$) but not P_{12} and P_{50}.

Influence of branch age on embolism resistance across the gradient

Although we carefully sampled branches of similar size across the gradient, a certain variation in BA per given A_{xylem} was observed (Fig. S1). This variation was unrelated to changes in MAP and thus not site-specific (Table 3). According to an LME model with BA added as a covariable or as a third random effect, MAP was still significantly related to all three measures of embolism resistance (covariable: $P < 0.01$; random effect: $P < 0.05$). We further removed the youngest and oldest branches from the data set, that is, the 15% extreme ages younger than 4 years and older than 9 years; this linear regression analysis supported the LME model with BA included as a covariable or random effect (Fig. S2a). Consequently, BA can be excluded as the principal driver of embolism resistance along the gradient.

Mutual interrelationships between traits

The interrelationships between hydraulic, wood anatomical and foliar traits revealed by the tree-level Pearson correlation analysis (Table 4) principally match the results of a PCA conducted with plot-level means. The first two principal components together explained 72% of the variance (Table 5). Axis 1 (eigenvalue 0.44) was strongly associated with MAP and all hydraulic and wood anatomical traits including foliar $\delta^{13}C$, but showed no relationship to K_L, P_{88} and the traits depending on sapwood area. These parameters and the foliar traits SLA and LS as well as G_{dw} were associated with axis 2. The plot-level analysis thus reveals relationships between climatic aridity, branch wood anatomical properties, hydraulic efficiency and embolism resistance that are closer than those found in the tree-level analysis shown in Table 4: neither hydraulic efficiency nor vessel diameter was related to embolism resistance at the tree level but such relationships became visible at the plot level (Fig. S3). Our differential analyses at the branch, tree and plot (stand) levels revealed that, for most functional traits, the largest variation existed among the branches within a tree, followed by the variance between the trees of a plot, while a much lower variation was detected between the five plots along the precipitation gradient (see Table S4). This suggested selecting the tree as the focal object of analysis and pooling over the replicate branches, while examining differences between plots in a second step.

Discussion

Climatic influences on wood anatomical, hydraulic and foliar traits

We observed a close relationship between MSP and D in similarly sized branches from the uppermost canopy of mature beech trees, partly supporting our first hypothesis which postulated that vessel diameter and hydraulic efficiency decrease with a lasting reduction in precipitation. The decline in D by 7% from the wet to the dry end of the gradient was nearly exclusively caused by shifts in the relative abundance of vessels with a diameter between 10 and 30 µm. In contrast, the three larger vessel diameter classes, which primarily consist of early-wood vessels and are of great importance for the calculation of D_h, were unaffected. As a consequence, D_h did not change across our precipitation gradient. The altered diameter pattern is also mirrored in the absence of any relationship between either MAP or MSP and K_P or K_S, because hydraulic conductivity increases with diameter raised to the fourth power according to the Hagen–Poiseuille law, and the diameter alteration in the 10–30 µm class is of low importance for K_P.

The functionality of the vascular system is best analysed in conjunction with the dependent foliage for understanding wood anatomical modifications in response to the environment

Table 4 Pearson correlation coefficients for linear relationships between 23 functional trait variables across trees in European beech (*Fagus sylvatica*)

	BA	K_S	K_P	K_L	P_{12}	P_{50}	P_{88}	WD	D	D_h	VD	VI	V_G	V_S	T_m	T_w	A_{xylem}	A_{xylem} : A_{leaf}	A_{lumen} : A_{xylem}	G_{dw}	LS	SLA
K_S	−0.52																					
K_P	ns	0.62																				
K_L	ns	0.47	ns																			
P_{12}	ns	ns	ns	ns																		
P_{50}	***0.34***	ns	ns	ns	0.91																	
P_{88}	0.49	ns	ns	ns	0.66	0.92																
WD	ns	ns	ns	ns	ns	ns	ns															
D	ns	0.60	0.87	***0.41***	ns	ns	ns	ns														
D_h	ns	0.56	0.90	ns	ns	ns	ns	ns	0.83													
VD	ns	ns	ns	ns	−0.46	***−0.34***	ns	−0.59	***−0.43***	ns												
VI	***−0.41***	***0.36***	***0.39***	ns	***0.40***	ns	ns	***0.44***	0.77	0.50	−0.87											
V_G	ns	ns	ns	ns	ns	ns	ns	ns	***−0.35***	ns	0.60	−0.57										
V_S	ns	ns	ns	ns	ns	ns	ns	ns	0.31	ns	−0.58	0.54	−0.95									
T_m	ns	ns	ns	ns	ns	ns	***−0.56***	ns	ns	ns	ns	ns	ns	ns								
T_w	ns	ns	ns	ns	ns	ns	ns	ns	ns	ns	ns	ns	ns	ns	***0.44***							
A_{xylem}	***0.37***	***−0.39***	ns	ns	***0.37***	0.47	0.49	ns	ns	ns	ns	ns	ns	ns	ns	ns						
A_{xylem} : A_{leaf}	ns	ns	***−0.40***	0.60	ns	ns	ns	ns	ns	−0.55	ns	ns	ns	ns	ns	ns	***0.34***					
A_{lumen} : A_{xylem}	ns	0.48	0.91	ns	ns	ns	ns	ns	0.67	0.71	ns	ns	ns	ns	ns	ns	ns	ns				
G_{dw}	−0.64	***0.44***	***0.44***	ns	ns	ns	***−0.34***	***0.40***	0.65	***0.44***	−0.49	0.70	ns	ns	ns	ns	ns	ns	ns			
LS	ns	ns	ns	***−0.40***	ns	ns	ns	ns	ns	***0.34***	ns	ns	ns	ns	ns	ns	ns	−0.68	ns	0.48		
SLA	ns	ns	ns	***−0.37***	ns	ns	ns	ns	ns	ns	ns	ns	ns	ns	ns	ns	ns	***−0.44***	ns	ns	0.55	
$\delta^{13}C$	***−0.34***	ns	ns	ns	ns	ns	ns	ns	ns	ns	−0.45	***0.42***	ns	ns	ns	ns	ns	ns	ns	***0.35***	ns	ns

ns, nonsignificant; bold and italic text, $P < 0.05$; bold text, $P < 0.01$; bold underlined text, $P < 0.001$. See Table 2 for definitions of abbreviations.

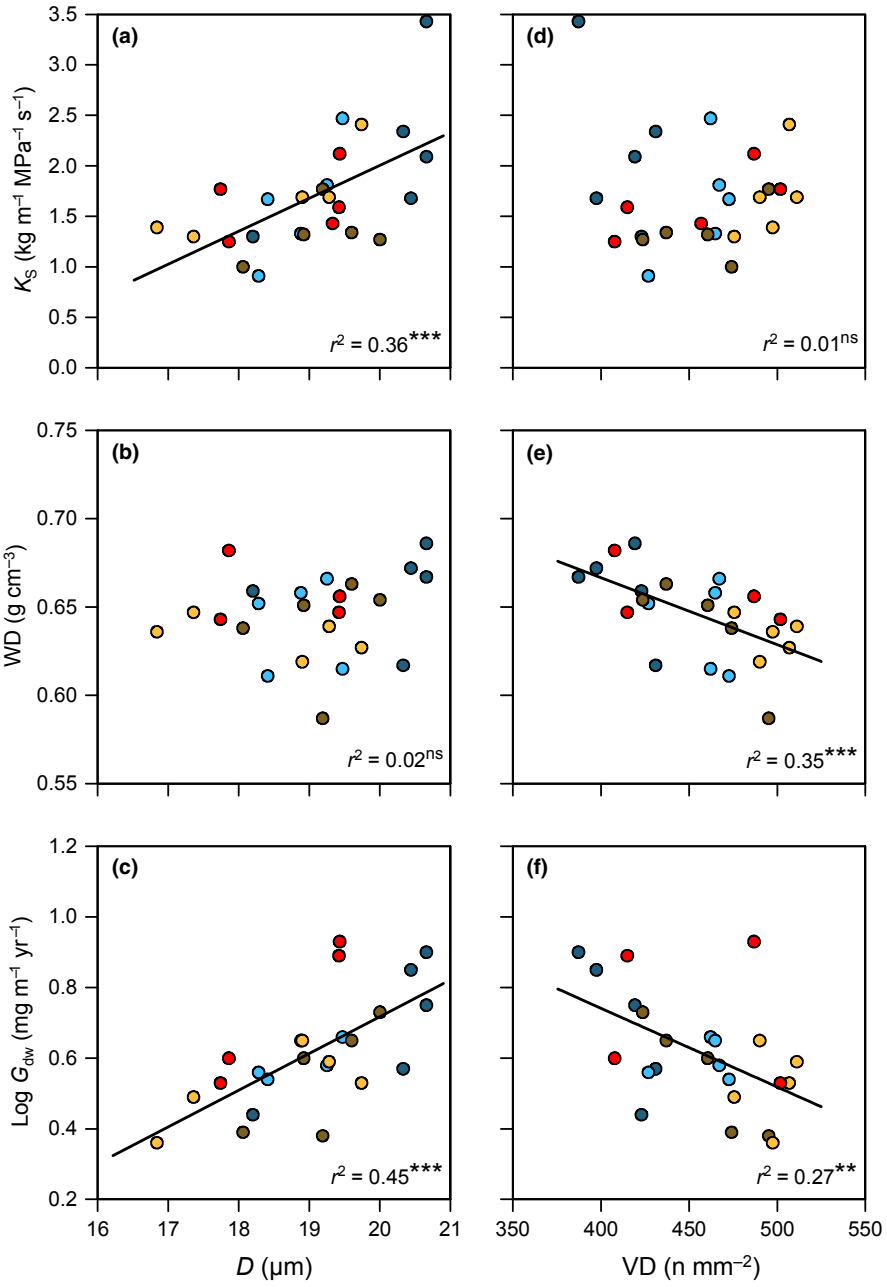

Fig. 4 Vessel diameter (D; left) and vessel density (VD; middle) in relation to specific conductivity (a, d; K_S), wood density (b, e; WD) and branch growth rate (c, f; G_{dw}) in European beech (*Fagus sylvatica*). Values are means per tree ($n = 25$); asterisks indicate the level of significance (**, $P < 0.01$; ***, $P < 0.001$; ns, nonsignificant relationships). For explanations of symbol colours, see Table 1.

(Carlquist, 2012). Both tissues related to water transport might have coevolved with respect to traits governing xylem vulnerability to embolism (Brodribb *et al.*, 2003; Nolf *et al.*, 2015). Although K_P and K_S remained more or less constant, K_L decreased unexpectedly by 40% with a MAP decrease of 260 mm yr^{-1}. Generally, K_L is supposed to increase in plants that are frequently exposed to drought in order to maintain a favourable leaf water status (Mencuccini & Grace, 1995; Sterck *et al.*, 2008). This is achieved either by an increase in K_S or more likely by adjustment of $A_{xylem} : A_{leaf}$. In Scots pine (*Pinus sylvestris*), for example, both K_L and $A_{xylem} : A_{leaf}$ increased with climate dryness across Europe, while K_S and D remained unchanged (Martinez-Vilalta *et al.*, 2009; Sterck *et al.*, 2012). This indicates that this coniferous species responds to increasing drought exposure mainly by reducing the supported leaf area per unit sapwood area. In beech, the decrease in K_L with a reduction in MAP along the gradient was caused by an increase in dependent leaf area towards the drier stands. By contrast, most other studies found an increase in $A_{xylem} : A_{leaf}$ with increasing climatic aridity, both within and between species (Poyatos *et al.*, 2007; Gleason *et al.*, 2013). Along our gradient, however, mean leaf size tended to increase, and not decrease, towards the drier eastern stands as also observed by Meier & Leuschner (2008) in a precipitation gradient of beech forests on sandstone in Central Germany.

A major finding of this study is that embolism resistance increased in parallel with declining D with increasing climatic aridity across our gradient, supporting our second hypothesis. To

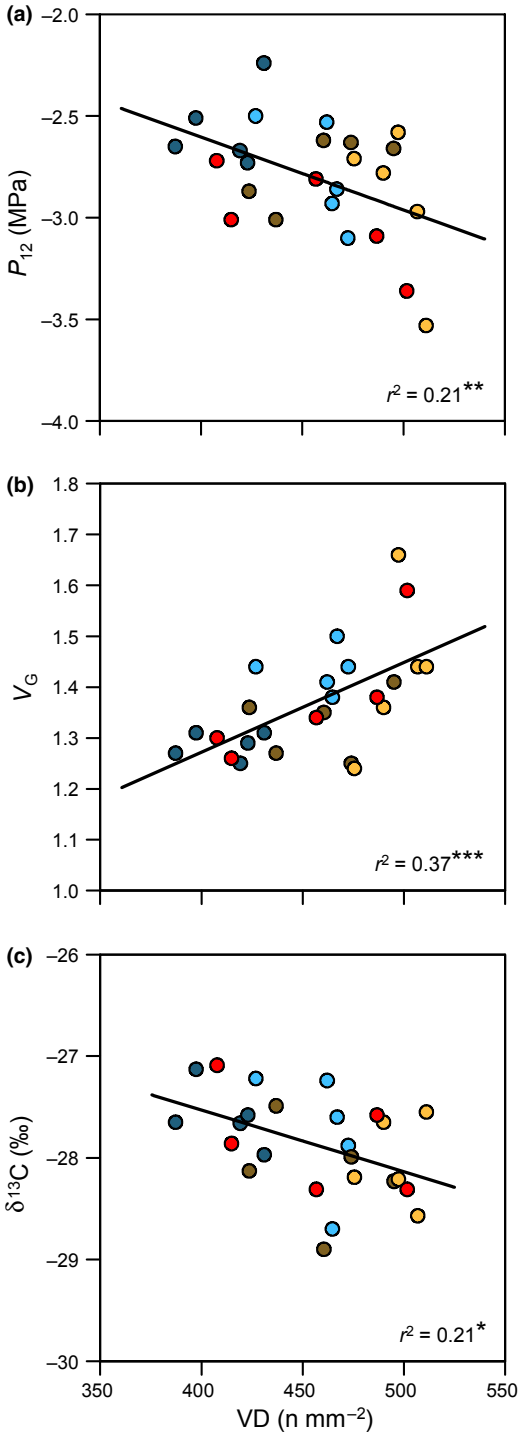

Fig. 5 (a) Xylem pressure causing 12% loss of hydraulic conductance (P_{12}), (b) vessel grouping index (V_G) and (c) carbon isotope signature ($\delta^{13}C$) in relation to vessel density (VD) in European beech (*Fagus sylvatica*). Values are means per tree ($n = 25$); asterisks indicate the level of significance (*, $P < 0.05$; **, $P < 0.01$; ***, $P < 0.001$). For explanations of symbol colours, see Table 1.

our knowledge, this is the first study demonstrating a linear intraspecific increase in embolism resistance with increasing drought stress. This finding provides additional support for the assumption that *F. sylvatica* is highly plastic with respect to embolism resistance (Herbette *et al.*, 2010), and that embolism resistance is under environmental rather than genetic control in this angiosperm tree species (Wortemann *et al.*, 2011). In *P. sylvestris* and *Pinus pinaster*, by contrast, P_{50} was unrelated to climatic aridity (Martinez-Vilalta *et al.*, 2009; Lamy *et al.*, 2014). These contrasting results might be explained by the observation that populations of angiosperm tree species generally possess a higher intraspecific variation in hydraulic traits than conifers (Anderegg, 2015). However, one has to keep in mind that vessel diameter, hydraulic properties and embolism resistance are influenced not only by the moisture regime but certainly also by other biotic and environmental factors, which complicates the interpretation of results obtained from climatic gradients. It has been shown that tree size and sampling height (Lintunen & Kalliokoski, 2010; Anfodillo *et al.*, 2013), as well as soil properties, in particular nutrient availability (Goldstein *et al.*, 2013) and water storage capacity (Tokumoto *et al.*, 2014), strongly influence the hydraulic architecture of plants. In cross-regional comparisons, it is therefore mandatory to keep tree size (or age) and soil properties as constant as possible in order to detect effects of environmental factors.

The observed modification of the hydraulic system across our precipitation gradient indicates that trees growing at the dry end tolerate more negative stem water potentials before water transport to the canopy is impeded. That this hydraulic adaptation was effective with respect to the maintenance of leaf gas exchange under drier conditions is suggested by the invariance of leaf $\delta^{13}C$ across the precipitation gradient.

Relationships between wood properties and embolism resistance

One of the principal hypotheses of plant hydraulics postulates a general trade-off between hydraulic safety and efficiency. This hypothesis is not confirmed by our data, which is in line with the majority of studies recently summarized by Gleason *et al.* (2016). Although both D and the three measures of embolism vulnerability decreased with climatic aridity and a close relationship between D and hydraulic efficiency was observed, neither D nor K_S was related to xylem safety. Tyree & Sperry (1989) argued that D is not directly related to the mechanism of embolism formation but rather results from a correlation with pit membrane pore size. Nevertheless, several studies have demonstrated this close, albeit presumably indirect, relationship among and across species (Wheeler *et al.*, 2005; Maherali *et al.*, 2006; Domec *et al.*, 2010; Hajek *et al.*, 2014). We assume that the range of variation in D and P_{50} was too small to confirm this relationship across the trees in our intraspecific study. Instead, VD was closely related to the air-entry point of embolism formation (P_{12}) but not to hydraulic efficiency. The V_G was likewise associated with P_{12} (although at marginal significance only) and closely related to VD, as observed by Lens *et al.* (2011). These results are in line with Carlquist's (1966) assumption that vessels should group to a larger degree in species adapted to water-limited environments with a xylem tissue composed of nonconductive fibres and no vasicentric tracheids; this would enable the maintenance of the

Table 5 Results of a principal components analysis (PCA) on the relationships between various climatic, hydraulic, woody and foliar traits (means of the five investigated study sites) and the eigenvalues of the four main axes in European beech (*Fagus sylvatica*)

Variables	Axis 1 EV 0.44	Axis 2 EV 0.28	Axis 3 EV 0.18	Axis 4 EV 0.10
Environmental conditions				
MAP	**0.75 (0.56)**	0.64 (0.97)	−0.14 (0.99)	0.08 (1.00)
Structural parameters				
BA	−0.51 (0.26)	0.34 (0.38)	**0.77 (0.97)**	−0.18 (1.00)
Hydraulic traits				
K_S	**0.73 (0.53)**	−0.17 (0.56)	−0.58 (0.89)	0.32 (1.00)
K_P	**0.78 (0.61)**	−0.36 (0.74)	0.40 (0.91)	0.30 (1.00)
K_L	0.30 (0.09)	**0.95 (0.99)**	0.05 (1.00)	0.07 (1.00)
P_{12}	**0.88 (0.77)**	0.39 (0.92)	0.17 (0.95)	0.22 (1.00)
P_{50}	**0.79 (0.62)**	0.61 (0.99)	0.09 (1.00)	−0.02 (1.00)
P_{88}	0.57 (0.32)	**0.77 (0.91)**	−0.01 (0.91)	−0.29 (1.00)
Wood properties				
WD	**0.70 (0.49)**	−0.58 (0.82)	−0.23 (0.88)	−0.35 (1.00)
D	**0.99 (0.97)**	0.00 (0.97)	0.16 (1.00)	0.02 (1.00)
D_h	**0.76 (0.57)**	−0.51 (0.83)	0.41 (1.00)	−0.02 (1.00)
VD	**−0.95 (0.90)**	0.11 (0.91)	−0.01 (0.91)	0.30 (1.00)
VI	**0.98 (0.96)**	−0.03 (0.96)	0.01 (0.96)	−0.19 (1.00)
V_G	**−0.81 (0.65)**	0.34 (0.77)	−0.48 (1.00)	−0.03 (1.00)
V_S	**0.73 (0.54)**	−0.35 (0.66)	0.58 (1.00)	0.05 (1.00)
T_m	**−0.84 (0.71)**	−0.53 (0.99)	−0.06 (1.00)	−0.04 (1.00)
T_w	0.45 (0.20)	−0.23 (0.25)	**−0.84 (0.96)**	0.21 (1.00)
A_{xylem}	−0.04 (0.00)	0.44 (0.20)	**0.73 (0.73)**	−0.52 (1.00)
$A_{xylem} : A_{leaf}$	−0.17 (0.03)	**0.86 (0.78)**	−0.32 (0.88)	−0.34 (1.00)
$A_{lumen} : A_{xylem}$	0.21 (0.04)	−0.17 (0.07)	0.66 (0.51)	**0.70** (1.00)
G_{dw}	0.55 (0.30)	**−0.62 (0.68)**	−0.19 (0.72)	−0.53 (1.00)
Foliar traits				
LS	−0.09 (0.01)	**−0.99 (0.98)**	−0.14 (1.00)	0.04 (1.00)
SLA	−0.13 (0.02)	**−0.66 (0.45)**	0.34 (0.57)	−0.66 (1.00)
$\delta^{13}C$	**0.68 (0.47)**	0.04 (0.47)	−0.69 (0.94)	−0.24 (1.00)

The cumulative coefficient of determination is given in parentheses. Numbers in bold indicate the variable with the closest correlation to the respective axis. See Table 2 for definitions of abbreviations.

conductive flow path by pathway redundancy if the largest vessel of the group embolizes. Through such vascular modification with more and to a higher degree grouped vessels in order to lower the xylem pressure at the onset of embolism formation, trees are presumably able to tolerate more negative leaf water potentials before stomata have to be closed. This assumption is supported by our negative relationship between VD and foliar $\delta^{13}C$. It has further been shown that stomatal closure correlates with the entry point of embolism formation in angiosperms, that is, the P_{12} value (Nardini *et al.*, 2001; Cochard *et al.*, 2002).

In contrast to VD and V_G, T_m correlated best with the xylem pressure inducing 88% loss of hydraulic conductance (P_{88}), although a marginally significant relationship also existed with P_{50}. It has been shown that the thickness of the membrane in angiosperm xylem is directly related to its maximum pore diameter (Jansen *et al.*, 2009b), making air-seeding more likely for thin membranes (Wheeler *et al.*, 2005). However, this does not explain why in our sample the closest relationship existed to the most negative pressure at P_{88}. It is likely that there are still serious gaps in our mechanistic understanding of air-seeding in plants (Schenk *et al.*, 2015).

For three other traits often associated with embolism resistance, namely WD, $A_{xylem} : A_{leaf}$ and specific leaf area, we were not able to confirm such a relationship in our data set. Such relationships may become visible only in data sets spanning different species or in intraspecific studies with much greater site and trait variation than is encountered in our precipitation gradient. Other biological properties may also influence embolism resistance, notably branch age, as we found older branches to be most vulnerable to cavitation, in agreement with Domec *et al.* (2009). However, we believe that this effect is primarily caused by cavitation fatigue, that is, the reduction of cavitation pressure as a consequence of previous cavitation in older xylem elements (Hacke *et al.*, 2001), even though we corrected for the potential bias of fatigue by applying a certain pressure before the onset of conductivity measurements (Jacobsen *et al.*, 2007). Further research is needed to show how many growth rings of older branches remain conductive in angiosperm trees (but see Christensen-Dalsgaard & Tyree, 2014) and to clarify whether sample flushing before the construction of vulnerability curves introduces measuring artefacts.

Relationship between hydraulic efficiency and branch growth

Similar to Sterck *et al.* (2012), we use sun-canopy G_{dw} as a measure of productivity because a dependence of growth on branch

hydraulics is more likely at this level than for stem wood or total aboveground productivity. In our study, faster growing younger branches of similar size to older ones possessed a more efficient hydraulic system and supported larger leaves, which subsequently caused more frequent stomatal closure. This finding is in agreement with our third hypothesis assuming a close relationship between hydraulic efficiency and growth, which might trade off with embolism resistance (Cochard *et al.*, 2007).

Unexpected is our finding that older slower growing branches in a given diameter class were more vulnerable than younger faster growing branches, as is indicated by the negative relationship between G_{dw} and P_{88}. Generally, fast growth is associated with larger vessels that cause higher hydraulic efficiency, which should result in a relatively vulnerable xylem (Hajek *et al.*, 2014). Although all branches investigated originated from the uppermost sun-exposed canopy, we assume that the older and the slower growing branches of similar size have not been exposed to full sunlight and thus to high atmospheric demand in the past, presumably because they were shaded by younger fast-growing branches. A similar pattern was observed by Herbette *et al.* (2010) when comparing sun-exposed and deeply shaded beech branches; the latter were on average 50% more vulnerable. This high variability in xylem embolism resistance, even at the same canopy position, is strong support for the frequently claimed high phenotypic plasticity in the morphology and physiology of European beech (Herbette *et al.*, 2010; Bresson *et al.*, 2011; Wortemann *et al.*, 2011). Shade-tolerant beech trees produce leaves that tolerate either full sunlight or deep shade and it can be assumed that this great plasticity in leaf function is also reflected in the hydraulic system of branches and petioles. However, given that G_{dw} was not related to any other parameter of embolism resistance in our study, it is premature to conclude that a trade-off between embolism resistance and branch growth does exist in the beech trees of our study. In agreement with this assumption, several other studies failed to detect relationships between vulnerability and growth (Sterck *et al.*, 2012; Hajek *et al.*, 2014; Guet *et al.*, 2015), indicating that embolism resistance is partly decoupled from hydraulic efficiency and biomass production (Fichot *et al.*, 2015).

Conclusions

In the sun canopy of beech trees, morphological adjustment to permanently reduced precipitation seems to occur primarily through the development of more cavitation-resistant branch wood, and not through a reduction of the supported leaf area. As a result of this modification, trees at the dry end of the gradient are capable of tolerating 15% more negative stem water potentials before the onset of cavitation. Our results show that the branch hydraulic system of beech has a considerable adaptive potential to respond to the local climatic conditions. This finding is strong evidence in support of the assumption that embolism resistance is largely under environmental control in this angiosperm tree species. It remains unclear, however, whether the observed hydraulic variability at the branch level can fully buffer against constraints imposed on growth and vitality by a warming and drying climate. Over the last three to four decades, a radial growth decline has been observed in those beech stands of our study region that are exposed to less than *c.* 635 mm yr^{-1} precipitation. This casts doubt on the capability of *F. sylvatica* to withstand increased drought and warming stress in the future solely through its flexible hydraulic response.

Acknowledgements

We thank Andre Meier and Tobias Fochler (BaumDirekt) for sample collection from the uppermost canopy with tree-climbing equipment, Claus Döring for providing meteorological data, and Ina Meier for support with data on leaf morphology as well as all involved technical and student assistants for their invaluable help in collecting and processing this data set. This study is part of the research programme 'Climate Impact and Adaptation Research in Lower Saxony (KLIFF)'. Financial support from the Ministry of Science and Culture of Lower Saxony received by C.L. is gratefully acknowledged. S.J. acknowledges technical support from the Electron Microscopy Section (Ulm University) for the preparation of TEM samples. Constructive and helpful comments from three anonymous reviewers and the handling editor helped to improve the manuscript.

Author contributions

B.S. and C.L. designed the study, F.K. collected the field samples, F.K., B.S., R.B. and S.D. measured and analysed the vulnerability curves, S.J. carried out the TEM observations and B.S. the wood anatomical measurements, H.M-H. contributed climatic and structural data, Y.C., B.S. and S.D. performed the statistical analyses and B.S., F.K. and C.L. wrote the first version of the manuscript, which was intensively discussed and revised by all authors.

References

Anderegg WRL. 2015. Spatial and temporal variation in plant hydraulic traits and their relevance for climate change impacts on vegetation. *New Phytologist* **205**: 1008–1014.

Anderegg WRL, Flint A, Huang C, Flint L, Berry JA, Davis FW, Sperry JS, Field CB. 2015. Tree mortality predicted from drought-induced vascular damage. *Nature Geoscience* **8**: 367–371.

Anderegg WRL, Meinzer FC. 2015. Wood anatomy and plant hydraulics in a changing climate. In: Hacke U, ed. *Functional and ecological xylem anatomy.* Cham, Switzerland: Springer International Publishing, 235–253.

Anfodillo T, Petit G, Crivellaro A. 2013. Axial conduit widening in woody species: a still neglected anatomical pattern. *IAWA Journal* **34**: 352–364.

Aranda I, Cano FJ, Gasco A, Cochard H, Nardini A, Mancha JA, Lopez R, Sanchez-Gomez D. 2015. Variation in photosynthetic performance and hydraulic architecture across European beech (*Fagus sylvatica* L.) populations supports the case for local adaptation to water stress. *Tree Physiology* **35**: 34–46.

Bohn U, Neuhäusl R, Mitarbeit U. 2003. *Map of the natural vegetation of Europe. Scale 1:2500000.* Bonn, Germany: Bundesamt für Naturschutz (BfN)/Federal Agency for Nature Conservation.

Bolte A, Czajkowski T, Kompa T. 2007. The north-eastern distribution range of European beech: a review. *Forestry* **80**: 413–429.

Bouche PS, Larter M, Domec JC, Burlett R, Gasson P, Jansen S, Delzon S. 2014. A broad survey of hydraulic and mechanical safety in the xylem of conifers. *Journal of Experimental Botany* **65**: 4419–4431.

Bréda N, Huc R, Granier A, Dreyer E. 2006. Temperate forest trees and stands under severe drought: a review of ecophysiological responses, adaptation processes and long-term consequences. *Annals of Forest Science* **63**: 625–644.

Bresson CC, Vitasse Y, Kremer A, Delzon S. 2011. To what extent is altitudinal variation of functional traits driven by genetic adaptation in European oak and beech? *Tree Physiology* **31**: 1164–1174.

Brodribb TJ, Holbrook NM, Edwards EJ, Gutierrez MV. 2003. Relations between stomatal closure, leaf turgor and xylem vulnerability in eight tropical dry forest trees. *Plant, Cell & Environment* **26**: 443–450.

Carlquist S. 1966. Wood anatomy of compositae: a summary, with comments on factors controlling wood evolution. *Aliso* **6**: 25–44.

Carlquist S. 1977. Ecological factors in wood evolution – floristic approach. *American Journal of Botany* **64**: 887–896.

Carlquist S. 2012. How wood evolves: a new synthesis. *Botany-Botanique* **90**: 901–940.

Chenlemuge T, Schuldt B, Dulamsuren C, Hertel D, Leuschner C, Hauck M. 2015. Stem increment and hydraulic architecture of a boreal conifer (*Larix sibirica*) under contrasting macroclimates. *Trees–Structure and Function* **29**: 623–636.

Christensen-Dalsgaard KK, Tyree MT. 2014. Frost fatigue and spring recovery of xylem vessels in three diffuse-porous trees *in situ*. *Plant, Cell & Environment* **37**: 1074–1085.

Cochard H, Casella E, Mencuccini M. 2007. Xylem vulnerability to cavitation varies among poplar and willow clones and correlates with yield. *Tree Physiology* **27**: 1761–1767.

Cochard H, Coll L, Le Roux X, Ameglio T. 2002. Unraveling the effects of plant hydraulics on stomatal closure during water stress in walnut. *Plant Physiology* **128**: 282–290.

Cochard H, Damour G, Bodet C, Tharwat I, Poirier M, Ameglio T. 2005. Evaluation of a new centrifuge technique for rapid generation of xylem vulnerability curves. *Physiologia Plantarum* **124**: 410–418.

De Micco V, Aronne G, Baas P. 2008. Wood anatomy and hydraulic architecture of stems and twigs of some Mediterranean trees and shrubs along a mesic–xeric gradient. *Trees–Structure and Function* **22**: 643–655.

Delzon S, Douthe C, Sala A, Cochard H. 2010. Mechanism of water-stress induced cavitation in conifers: bordered pit structure and function support the hypothesis of seal capillary-seeding. *Plant, Cell & Environment* **33**: 2101–2111.

Domec J-C, Gartner BL. 2001. Cavitation and water storage capacity in bole xylem segments of mature and young Douglas-fir trees. *Trees* **15**: 204–214.

Domec J-C, Schafer K, Oren R, Kim HS, McCarthy HR. 2010. Variable conductivity and embolism in roots and branches of four contrasting tree species and their impacts on whole-plant hydraulic performance under future atmospheric CO_2 concentration. *Tree Physiology* **30**: 1001–1015.

Domec J-C, Warren JM, Meinzer FC, Lachenbruch B. 2009. Safety factors for xylem failure by implosion and air-seeding within roots, trunks and branches of young and old conifer trees. *IAWA Journal* **30**: 101–120.

Eilmann B, Sterck F, Wegner L, de Vries SMG, von Arx G, Mohren GMJ, den Ouden J, Sass-Klaassen U. 2014. Wood structural differences between northern and southern beech provenances growing at a moderate site. *Tree Physiology* **34**: 882–893.

Ellenberg H, Leuschner C. 2010. *Vegetation Mitteleuropas mit den Alpen in ökologischer, dynamischer und historischer Sicht, 6th edn*. Stuttgart, Germany: Ulmer.

Fan DY, Jie SL, Liu CC, Zhang XY, Xu XW, Zhang SR, Xie ZQ. 2011. The trade-off between safety and efficiency in hydraulic architecture in 31 woody species in a karst area. *Tree Physiology* **31**: 865–877.

Fichot R, Brignolas F, Cochard H, Ceulemans R. 2015. Vulnerability to drought-induced cavitation in poplars: synthesis and future opportunities. *Plant, Cell & Environment* **38**: 1233–1251.

Fischer EM, Schär C. 2008. Future changes in daily summer temperature variability: driving processes and role for temperature extremes. *Climate Dynamics* **33**: 917–935.

Führer E, Horváth L, Jagodics A, Machon A, Szabados I. 2011. Application of a new aridity index in Hungarian forestry practice. *Idojaras* **115**: 205–216.

Gessler A, Keitel C, Kreuzwieser J, Matyssek R, Seiler W, Rennenberg H. 2007. Potential risks for European beech (*Fagus sylvatica* L.) in a changing climate. *Trees – Structure and Function* **21**: 1–11.

Gleason SM, Butler DW, Waryszak P. 2013. Shifts in leaf and stem hydraulic traits across aridity gradients in Eastern Australia. *International Journal of Plant Sciences* **174**: 1292–1301.

Gleason SM, Butler DW, Ziemińska K, Waryszak P, Westoby M. 2012. Stem xylem conductivity is key to plant water balance across Australian angiosperm species. *Functional Ecology* **26**: 343–352.

Gleason SM, Westoby M, Jansen S, Choat B, Hacke UG, Pratt RB, Bhaskar R, Brodribb TJ, Bucci SJ, Cao KF *et al.* 2016. Weak tradeoff between xylem safety and xylem-specific hydraulic efficiency across the world's woody plant species. *New Phytologist* **209**: 123–136.

Goldstein G, Bucci SJ, Scholz FG. 2013. Why do trees adjust water relations and hydraulic architecture in response to nutrient availability? *Tree Physiology* **33**: 238–240.

Guet J, Fichot R, Ledee C, Laurans F, Cochard H, Delzon S, Bastien C, Brignolas F. 2015. Stem xylem resistance to cavitation is related to xylem structure but not to growth and water-use efficiency at the within-population level in *Populus nigra* L. *Journal of Experimental Botany* **66**: 4643–4652.

Hacke UG, Sperry JS, Pockman WT, Davis SD, McCulloch KA. 2001. Trends in wood density and structure are linked to prevention of xylem implosion by negative pressure. *Oecologia* **126**: 457–461.

Hajek P, Leuschner C, Hertel D, Delzon S, Schuldt B. 2014. Trade-offs between xylem hydraulic properties, wood anatomy and yield in *Populus*. *Tree Physiology* **34**: 744–756.

Herbette S, Wortemann R, Awad H, Huc R, Cochard H, Barigah TS. 2010. Insights into xylem vulnerability to cavitation in *Fagus sylvatica* L.: phenotypic and environmental sources of variability. *Tree Physiology* **30**: 1448–1455.

Hertel D, Strecker T, Müller-Haubold H, Leuschner C. 2013. Fine root biomass and dynamics in beech forests across a precipitation gradient – is optimal resource partitioning theory applicable to water-limited mature trees? *Journal of Ecology* **101**: 1183–1200.

Hoeber S, Leuschner C, Köhler L, Arias-Aguilar D, Schuldt B. 2014. The importance of hydraulic conductivity and wood density to growth performance in eight tree species from a tropical semi-dry climate. *Forest Ecology and Management* **330**: 126–136.

Jacob D, Göttel H, Kotlarski S, Lorenz P, Sieck K. 2008. Klimaauswirkungen und Anpassung in Deutschland – Phase 1: Erstellung regionaler Klimaszenarien für Deutschland. In: Umweltbundesamt, eds. *Reihe climate change*. 11/2008, ISSN 1862-4359, Dessau-Roßlau, Germany. [WWW document] URL http://www.umweltbundesamt.de/publikationen/klimaauswirkungen-anpassung-in-deutschland.

Jacobsen AL, Pratt RB, Ewers FW, Davis SD. 2007. Cavitation resistance among 26 chaparral species of southern California. *Ecological Monographs* **77**: 99–115.

Jansen S, Choat B, Pletsers A. 2009a. Morphological variation of intervessel pit membranes and implications to xylem function in angiosperms. *American Journal of Botany* **96**: 409–419.

Jansen S, Dute RR, Plavcová L, Choat B. 2009b. *Preparation of material for TEM examination*. Prometheus Wiki, CSIRO Publishing. [WWW document] URL http://prometheuswiki.publish.csiro.au/tiki-index.php?page=Preparation+of+Material+for+TEM+Examination.

Jump AS, Hunt JM, Peñuelas J. 2006. Rapid climate change-related growth decline at the southern range edge of *Fagus sylvatica*. *Global Change Biology* **12**: 2163–2174.

Kotowska MM, Hertel D, Abou Rajab Y, Barus H, Schuldt B. 2015. Patterns in hydraulic architecture from roots to branches in six tropical tree species from cacao agroforestry and their relation to wood density and stem growth. *Frontiers in Plant Science* **6**: 1–16.

Kremer A, Potts BM, Delzon S. 2014. Genetic divergence in forest trees: understanding the consequences of climate change. *Functional Ecology* **28**: 22–36.

Lamy JB, Delzon S, Bouche PS, Alia R, Vendramin GG, Cochard H, Plomion C. 2014. Limited genetic variability and phenotypic plasticity detected for cavitation resistance in a Mediterranean pine. *New Phytologist* **201**: 874–886.

Legendre P, Legendre L. 1998. *Numerical ecology, 2nd English edn*. Amsterdam, the Netherlands: Elsevier Science.

Lens F, Luteyn JL, Smets E, Jansen S. 2004. Ecological trends in the wood anatomy of Vaccinioideae (*Ericaceae* s.l.). *Flora – Morphology Distribution, Functional Ecology of Plants* **199**: 309–319.

Lens F, Sperry JS, Christman MA, Choat B, Rabaey D, Jansen S. 2011. Testing hypotheses that link wood anatomy to cavitation resistance and hydraulic conductivity in the genus *Acer*. *New Phytologist* **190**: 709–723.

Leuschner C. 2009. *Die Trockenheitsempfindlichkeit der Rotbuche vor dem Hintergrund des prognostizierten Klimawandels. Jahrbuch der Akademie der Wissenschaften zu Göttingen*. Berlin, Germany: Walter de Gruyter. [WWW document] URL adw-digital.sub.uni-goettingen.de/bitstream/handle/11858/00-001S-0000-0007-371C-7/Article-21.pdf?sequence=1.

Lewis AM, Boose ER. 1995. Estimating flow rates through xylem conduits. *American Journal of Botany* **82**: 1112–1116.

Lintunen A, Kalliokoski T. 2010. The effect of tree architecture on conduit diameter and frequency from small distal roots to branch tips in *Betula pendula*, *Picea abies* and *Pinus sylvestris*. *Tree Physiology* **30**: 1433–1447.

Loepfe L, Martinez-Vilalta J, Pinol J, Mencuccini M. 2007. The relevance of xylem network structure for plant hydraulic efficiency and safety. *Journal of Theoretical Biology* **247**: 788–803.

Maherali H, Moura CF, Caldeira MC, Willson CJ, Jackson RB. 2006. Functional coordination between leaf gas exchange and vulnerability to xylem cavitation in temperate forest trees. *Plant, Cell & Environment* **29**: 571–583.

Markesteijn L, Poorter L, Paz H, Sack L, Bongers F. 2011. Ecological differentiation in xylem cavitation resistance is associated with stem and leaf structural traits. *Plant, Cell & Environment* **34**: 137–148.

Martinez-Vilalta J, Cochard H, Mencuccini M, Sterck F, Herrero A, Korhonen JFJ, Llorens P, Nikinmaa E, Nole A, Poyatos R *et al.* 2009. Hydraulic adjustment of Scots pine across Europe. *New Phytologist* **184**: 353–364.

McDowell NG, Allen CD. 2015. Darcy's law predicts widespread forest mortality under climate warming. *Nature Climate Change* **5**: 669–672.

Meier IC, Leuschner C. 2008. Leaf size and leaf area index in *Fagus sylvatica* forests: competing effects of precipitation, temperature, and nitrogen availability. *Ecosystems* **11**: 655–669.

Meinke I, Gerstner E, von Storch H, Marx A, Schipper H, Kottmeier C, Treffeisen R, Lemke P. 2010. Regionaler Klimaatlas Deutschland der Helmholtz-Gemeinschaft informiert im Internet über möglichen künftigen Klimawandel. *DMG Mitteilungen* **2**: 7–9.

Mencuccini M, Grace J. 1995. Climate influences the leaf area/sapwood area ratio in Scots pine. *Tree Physiology* **15**: 1–10.

Müller-Haubold H, Hertel D, Seidel D, Knutzen F, Leuschner C. 2013. Climate responses of aboveground productivity and allocation in *Fagus sylvatica*: a transect study in mature forests. *Ecosystems* **16**: 1498–1516.

Nardini A, Tyree MT, Salleo S. 2001. Xylem cavitation in the leaf of *Prunus laurocerasus* and its impact on leaf hydraulics. *Plant Physiology* **125**: 1700–1709.

Nolf M, Creek D, Duursma R, Holtum J, Mayr S, Choat B. 2015. Stem and leaf hydraulic properties are finely coordinated in three tropical rainforest tree species. *Plant, Cell & Environment* **38**: 2652–2661.

Ogasa M, Miki NH, Murakami Y, Yoshikawa K. 2013. Recovery performance in xylem hydraulic conductivity is correlated with cavitation resistance for temperate deciduous tree species. *Tree Physiology* **33**: 335–344.

Pammenter NW, Vander Willigen C. 1998. A mathematical and statistical analysis of the curves illustrating vulnerability of xylem to cavitation. *Tree Physiology* **18**: 589–593.

Plavcová L, Jansen S, Klepsch M, Hacke UG. 2013. Nobody's perfect: can irregularities in pit structure influence vulnerability to cavitation? *Frontiers in Plant Science* **4**: 453.

Poyatos R, Martínez-Vilalta J, Cermák J, Ceulemans R, Granier A, Irvine J, Köstner B, Lagergren F, Meiresonne L, Nadezhdina N *et al.* 2007. Plasticity in hydraulic architecture of Scots pine across Eurasia. *Oecologia* **153**: 245–259.

R Development Core Team. 2013. *R: A language and environment for statistical computing*. Vienna, Austria: R Foundation for Statistical computing. URL http://www.R-project.org.

Rigling A, Bigler C, Eilmann B, Feldmeyer-Christe E, Gimmi U, Ginzler C, Graf U, Mayer P, Vacchiano G, Weber P *et al.* 2013. Driving factors of a vegetation shift from Scots pine to pubescent oak in dry Alpine forests. *Global Change Biology* **19**: 229–240.

Rowell DP, Jones RG. 2006. Causes and uncertainty of future summer drying over Europe. *Climate Dynamics* **27**: 281–299.

Schär C, Vidale PL, Lüthi D, Frei C, Häberli C, Liniger MA, Appenzeller C. 2004. The role of increasing temperature variability in European summer heatwaves. *Nature* **427**: 332–336.

Schenk HJ, Steppe K, Jansen S. 2015. Nanobubbles: a new paradigm for air-seeding in xylem. *Trends in Plant Science* **20**: 199–205.

Scholz A, Klepsch M, Karimi Z, Jansen S. 2013. How to quantify conduits in wood? *Frontiers in Plant Science* **4**: 56.

Schreiber SG, Hacke UG, Hamann A. 2015. Variation of xylem vessel diameters across a climate gradient: insight from a reciprocal transplant experiment with a widespread boreal tree. *Functional Ecology* **29**: 1392–1401.

Sperry JS, Nichols KL, Sullivan JEM, Eastlack SE. 1994. Xylem embolism in ring-porous, diffuse-porous, and coniferous trees of Northern Utah and Interior Alaska. *Ecology* **75**: 1736–1752.

Sterck FJ, Martínez-Vilalta J, Mencuccini M, Cochard H, Gerrits P, Zweifel R, Herrero A, Korhonen JFJ, Llorens P, Nikinmaa E *et al.* 2012. Understanding trait interactions and their impacts on growth in Scots pine branches across Europe. *Functional Ecology* **26**: 541–549.

Sterck FJ, Zweifel R, Sass-Klaassen U, Chowdhury Q. 2008. Persisting soil drought reduces leaf specific conductivity in Scots pine (*Pinus sylvestris*) and pubescent oak (*Quercus pubescens*). *Tree Physiology* **28**: 529–536.

Tokumoto I, Heilman JL, Schwinning S, McInnes KJ, Litvak ME, Morgan CLS, Kamps RH. 2014. Small-scale variability in water storage and plant available water in shallow, rocky soils. *Plant and Soil* **385**: 193–204.

Tyree MT. 2003. Hydraulic limits on tree performance: transpiration, carbon gain and growth of trees. *Trees–Structure and Function* **17**: 95–100.

Tyree MT, Davis SD, Cochard H. 1994. Biophysical perspectives of xylem evolution – is there a trade-off of hydraulic efficiency for vulnerability to dysfunction? *IAWA Journal* **15**: 335–360.

Tyree MT, Sperry JS. 1989. Vulnerability of xylem to cavitation and embolism. *Annual Review of Plant Physiology and Plant Molecular Biology* **40**: 19–38.

Tyree MT, Zimmermann MH. 2002. *Xylem structure and the ascent of sap*. Berlin, Germany: Springer.

Vesque J. 1876. Note sur l'anatomie du *Goodenia ovate*. *Annales des Sciences Naturalles-Botanique et Biologie Vegetale* **6**: 312–326.

Weber P, Bugmann H, Pluess AR, Walthert L, Rigling A. 2013. Drought response and changing mean sensitivity of European beech close to the dry distribution limit. *Trees – Structure and Function* **27**: 171–181.

Wheeler JK, Sperry JS, Hacke UG, Hoang N. 2005. Inter-vessel pitting and cavitation in woody Rosaceae and other vesselled plants: a basis for a safety versus efficiency trade-off in xylem transport. *Plant, Cell & Environment* **28**: 800–812.

Willson CJ, Manos PS, Jackson RB. 2008. Hydraulic traits are influenced by phylogenetic history in the drought-resistant, invasive genus *Juniperus* (Cupressaceae). *American Journal of Botany* **95**: 299–314.

Wortemann R, Herbette S, Barigah TS, Fumanal B, Alia R, Ducousso A, Gomory D, Roeckel-Drevet P, Cochard H. 2011. Genotypic variability and phenotypic plasticity of cavitation resistance in *Fagus sylvatica* L. across Europe. *Tree Physiology* **31**: 1175–1182.

Zimmermann J, Hauck M, Dulamsuren C, Leuschner C. 2015. Climate warming-related growth decline affects *Fagus sylvatica*, but not other broad-leaved tree species in Central European mixed forests. *Ecosystems* **1**: 560–572.

Supporting Information

Additional supporting information may be found in the online version of this article.

Fig. S1 Variation in basipetal maximal branch diameter and branch age in European beech along the precipitation gradient, and relationship between branch age and basipetal xylem area.

Fig. S2 Mean annual precipitation in relation to P_{12}, P_{50} and P_{88} in European beech branches with an age between 4 and 9 yr, and branch age in relation to P_{50} for a given branch age class.

Fig. S3 Relationship between P_{12}, P_{50} and P_{88} in European beech branches and four traits commonly associated with embolism resistance at the tree and plot levels.

Table S1 Relationship between specific conductivity normalized to different positions along the branch segments and six wood anatomical and hydraulic predictors

Table S2 Summary of all major variables explored

Table S3 Results of linear mixed effects models of the influence of water availability on the relative abundance of vessels of five different vessel diameter classes

Table S4 Coefficient of variation of all traits measured for the variance between plots, between trees within a plot, and within a given tree

Please note: Wiley Blackwell are not responsible for the content or functionality of any supporting information supplied by the authors. Any queries (other than missing material) should be directed to the *New Phytologist* Central Office.